APS 2-ID BEAMLINE, UPGRADE TO CANTED CONFIGURATION *

D. Capatina†, M. Beno, M. Fisher, J. Knopp, B. Lai, E. Moog, C. Roehrig, S. Vogt,
Advanced Photon Source, Argonne National Laboratory, Lemont, USA

Abstract

To provide independent operation of the two 2-ID beamline experimental stations, a new canted beamline design is being developed. The constraint of keeping the existing front end limits the canting angle. The optimal canting angle was determined to be 400 µrad and is achieved by using a permanent magnet. A coil is added to the canting magnet to provide a steering adjustment of maximum 40 to 50 µrad. In order to increase the beam separation as well as to provide power filtering and higher harmonics rejection for the downstream optics, a dual mirror system with focusing capability is used as the first optic at approximately 28 m from the center of the straight section. The inboard mirror (2.6 mrad) reflects the inboard beam outboard while the outboard mirror (4.1 mrad) reflects the outboard beam inboard. The beam presented to the dual mirror system is defined by two 1 mm x 1 mm apertures. The maximum power absorbed by each mirror is 200 W. Two vertically deflecting monochromators with minimum offset of 17 mm are located in the First Optical Enclosure on the outboard branch. The monochromator for the inboard branch is located in the corresponding experimental station.

BEAMLINE LAYOUT

The 2-ID beamline infrastructure consists of three existing shielded enclosures, three mini-hutches and shielded transport. The mini-hutches are existing as well and are relocated as needed. The shielded transport is a new design. The schematic layout of the major optical and shielding components is shown in Fig. 1.

SOURCE

The X-ray source for the beamline consists of two 2.4-m-long undulators with a period length of 3.3 cm (U33), one for each branch, located symmetrically about the center of the straight section. The period may be further optimized in the future.

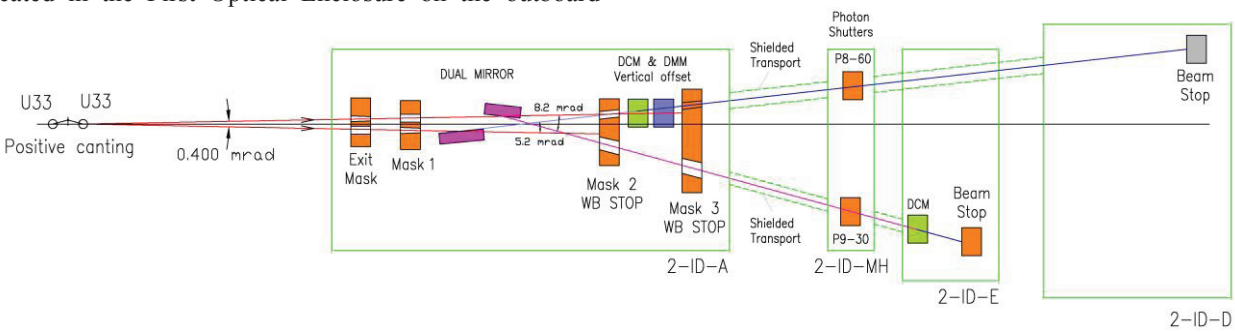

Figure 1: Schematic layout of the major optical and shielding components.

CANTING MAGNET

The design of the canting magnet for 2-ID is based on the permanent-magnet canting magnet planned for Sector 4-ID that introduces a bend of 400 µrad with a magnetic gap of 8.5 mm. Modifications are made to accommodate the larger vacuum chamber and larger magnetic gap in Sector 2. In addition, the ability to adjust the bend by a small amount is desired so the electron beam can be steered independently through the two undulators. A coil is added to the canting magnet to provide a steering adjustment of 40 to 50 µrad, maximum. That limitation on the steering adjustment avoids potential issues with power level increases on downstream masks. The cant centerline is offset 0.61 mm outboard of the traditional centerline (positive canting).

FRONT END

For cost reasons, the existing front end (FE), designed for inline operation, is kept in place, with a new exit mask and collimator. This constraint required that the canting angle be smaller than the typical APS canting angle of 1 mrad. The optimal angle for 2-ID was determined to be 400 µrad. In order for the FE masks and beam stops to remain within the design limits, the undulators cannot be set to their minimum gaps simultaneously. The output power of the undulators is limited to 6553 W. However, in designing the exit mask and the beamline heat absorbers, credit was not taken for the FE power limitation.

DUAL CANTING MIRROR

In order to increase the beam separation as well as to provide power filtering and higher-harmonics rejection for the downstream optics, a dual mirror system with focusing capability is used as the first optic at approximately 28 m from the center of the straight section.

Design Concept

The mirrors are mounted in a vacuum chamber, facing each other, in a staggered configuration, see Fig. 2. The mirror motions are completely independent of each other.

The inboard mirror (IM) with a nominal incident angle of 2.6 mrad reflects the inboard beam outboard while the outboard mirror (OM) with a nominal incident angle of 4.1 mrad reflects the outboard beam inboard. With the upgrade of the APS storage ring (APSU), all canting angles will be 1 mrad. To be able to continue using the Dual Canting Mirror, the system is provided with a one-time-change of the relative distance between the mirrors from 11.1 mm, for the current beamline configuration, to 28.0 mm after the APSU. This way the lateral translation is maintained to a small range of ± 6 mm for stability.

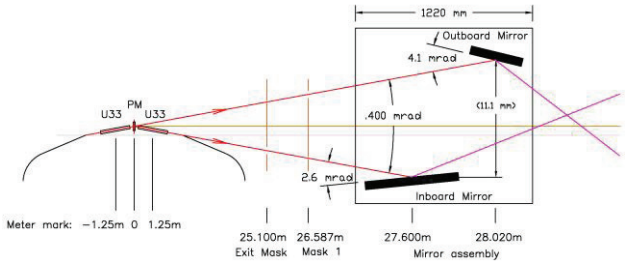

Figure 2: Schematic of the staggered mirror system.

The optical layout allows the beam separation to be between 38 mm and 56 mm at the monochromators.

To reduce the total power incident on the OM, the Exit Mask, located at 25.1 m, has a defining aperture of 1 mm x 1 mm, centered on the outboard white beam (WB). The inboard WB passes the Exit Mask through an aperture of 4 mm x 2 mm (HxV). Similarly, Mask 1 located at 26.5 m, has a defining aperture of 1 mm x 1 mm centered on the inboard WB, while the outboard WB passes through an aperture of 4 mm x 2 mm (HxV). Having the defining apertures in two separate masks assures the ease of manufacturing and alignment at installation.

Mirror Specifications

Each mirror has three reflecting surfaces: bare silicon substrate, rhodium, and platinum. Each mirror is provided with three motorized motions: X, Y, and pitch. The bending mechanism produces a surface figure that can be varied from flat to elliptical with minimal aberrations. The IM focuses horizontally onto a beam-defining aperture 6.25 m downstream, and the OM focuses horizontally onto a beam-defining aperture 6.43 m downstream. OM minimum bending radius is 2.6 km. IM minimum bending radius is 3.9 km. The white beam reaching each mirror is slightly over 1 mm^2 and the maximum power absorbed in each mirror is 208 W. The OM active length is 270 mm and the IM active length is 400 mm so that each mirror accepts the entire beam passing through the defining apertures.

Both mirrors are indirectly cooled to reduce vibrations via a typical "cooling slot and fin" design located at the top and bottom of the substrate. The Indium/Gallium eutectic is used as interface layer to enhance heat transfer. The meridional RMS slope error is expected to be ≤ 0.3 µrad and the RMS micro-roughness after coating ≤ 2.5 Å.

Compton scattering is a significant source of heat. When scattered radiation strikes a mirror support, the component could drift, resulting in a change of the mirror angle. The mirror supports therefore are designed to minimize exposure to scattered radiation, and are protected by shields. In addition, a shield is installed between the two mirrors to prevent Compton scattering produced by the IM from reaching the OM.

BEAMLINE SHIELDING COMPONENTS

The beamline shielding components consist of the masks, primary and secondary bremsstrahlung collimators located in the First Optics Enclosure (FOE), the photon shutters in the mini-hutch and the end station beam stops.

Collimators Specifications

Besides power filtering and suppression of high-order undulator harmonics, the dual canted mirror allows the separation of the bremsstrahlung radiation from the synchrotron radiation. The primary bremsstrahlung radiation is stopped at the end of the FOE by using the FE collimators and three beamline collimators, each one protected from the synchrotron beam by a mask. The task would have been achieved using two beamline collimators. By using an additional collimator, the minimum vertical offset of the monochromators located at the downstream end of the FOE has been reduced from 25 mm to 17 mm. In designing the secondary bremsstrahlung collimators (SBC), the OM was considered the worst scattering target in the FOE and the design follows the internal guidelines.

Masks Specifications

There are four masks in the beamline layout, all located in the FOE.

The **Exit Mask** intercepts the two canted WBs at full size in the horizontal (about 12 mm) and 7.2 mm in the vertical direction. In the worst case scenario, the canting angle is 350 µrad and the beams are overlapping at the Exit Mask by 3.2 mm and are 8.8 mm center to center. The beams cannot overlap at **Mask 1**, and the outboard beam passes through the outboard aperture in all mistering scenarios. Table 1 shows the total power and peak power density incident on each mask in the worst case scenario and the predicted maximum temperature (T_{max}) developed on the mask bodies. The Exit Mask is made of GlidCop, while Mask 1 is made of OFHC Copper. The power density distribution was calculated using SRUFF [1].

Table 1: WB Masks Key Parameters and T_{max}

Mask name	**Power** (W)	**Peak power density** (W/mm^2)	**Incident angle**	**T_{max}** (°C)
Exit M	9928	278	1.5°	259
Mask 1	977	248	2.0°	98

Mask 2, with an incident angle of 4°, is the first mask after the dual canting mirror. It intercepts the mistering cone of both focused pink beams (PBs), and stops the inboard WB and partially intercepts the outboard WB if either or both mirrors are retracted. Given the sources

listed above, the total PB power and size incident on the mask depends upon the mirror reflective stripe, incidence angle, total length and bend radius. Neither the limit switches, nor the possible hard stops of the mirrors' pitch are interlocked in the Personal Safety System and therefore Mask 2 was designed to handle the entire angular range [2]. For certain mirror angles the PB of one branch can overlap the WB of the other branch. Also, the PBs can overlap each other. The power calculation was conservative because it did not take into account the roughness of the mirrors, which could be below the specified value of 2.5 Å. The focused beam size was estimated as an ideal focal spot size with the Eq. (1):

$$F_{Ideal} = 2.35 \times \Sigma_{RMS} \times M \quad (1)$$

In Eq. (1) Σ_{RMS} is the RMS radiative source size and M is the demagnification. M = q/p, where q is the distance from mirror to image and p is the distance from source to mirror. Unlike Graber's calculations [3], the spherical aberration was neglected in this calculation because the mirror figure is expected to be very close to an elliptical shape. The fabrication slope error was neglected as well because the slope error of the actual mirrors might be smaller than the specified value of 0.3 μrad and the contribution of this error is very small. The OM and IM can focus onto Mask 2 for angles smaller than 1.8 mrad and 1.4 mrad, respectively. For larger incident angles and minimum bend radius, the mirrors will focus the beam downstream of Mask 2. In this case the beam size at Mask 2 was calculated using simple geometry. The relationship between the mirror bend radius (r), incidence angle (θ), p and q is defined by Eq. (2):

$$r = \frac{2}{(\frac{1}{p}+\frac{1}{q})\times\theta} \quad (2)$$

Several scenarios have been analysed and the maximum temperature (T_{max}) and von Mises stress (σ_{max}) were obtained when the smallest outboard PB was overlapping the outboard WB center. The IM incident angle was 1.9 mrad in this case. Table 2 shows beam size, power and peak power density of each beam for the worst loading case scenario.

Table 2: Mask 2 Worst Loading Case Scenario

Beam	Beam size		Power (W)	Peak power density (W/mm^2)
	H (mm)	V (mm)		
Outb WB	1.21	1.21	215.6	156.2
Outb PB	.399	1.16	109.7	237.0
Total			325.3	393.2

For OFHC Copper and a minimum water flow rate of 0.5 GPM, T_{max} was 126.9°C and σ_{max} was 111.1 MPa. The mask design is very simple and suitable for CuCrZr single-piece construction as described by Sharma [4]. For CuCrZr and the same flow rate, T_{max} was 146.3°C and σ_{max} was 142.8 MPa, which are well under the typical maximum values. The power of the PB striking outside of the mask body is very low (under 12.5 W) and doesn't present a safety issue.

Mask 3, with an incident angle of 7°, is the second mask after the dual mirror system and the first mask after the monochromators. It intercepts the mistering cone of the inboard PB, and stops the outboard WB and the outboard PB. Unlike Mask 2, the beams cannot overlap on Mask 3. The OM and IM incident angles of 3.6 mrad and 2.1 mrad, respectively, are the minimum angles for which the PBs pass downstream through the Mask 2 apertures. The mirrors can focus onto Mask 3 at these angles. The worst loading case is when Mask 3 intercepts the outboard WB and outboard PB. The beam parameters are in the same range as those in Table 2 with the main difference being the horizontal PB size of 0.166 mm. The T_{max} and σ_{max} are also well below the typical values and the mask is suitable for CuCrZr single-piece construction.

Photon Shutters and Beam Stops Specifications

The PB Photon Shutter absorber as well as the PB End Station Beam Stop have normal incidence to the beam. There is no significant demagnification of the beam in the horizontal direction at these devices and therefore the peak power density is relatively low (49 W/mm^2 at the Photon Shutter). The T_{max} and σ_{max} are well below the typical values. The Monochromatic Beam Photon Shutter and the End Station Beam Stop consist of Tungsten and Lead, respectively. The heat load output of the DMM is under 1 W.

CONCLUSION

The productivity of the 2-ID beamline will increase significantly with the canted configuration. The final design is ongoing. The installation of the 2-ID canted beamline will take place during the January 2018 shutdown followed by commissioning in March 2018.

REFERENCES

[1] Mati Meron, CARS_CAT, "SRUFF: A Comprehensive Package for Synchrotron Radiation Spectral and Optics Calculations", unpublished, 2001.

[2] D. Capatina *et al*., "DCS - A High Flux Beamline for Time Resolved Dynamic Compression Science – Design Highlights", Proceedings SRI Conf. (SRI2015), New York, USA, July 2015.

[3] T. Graber *et al.*, "BioCARS: a synchrotron resource for time-resolved X-ray science", *Journal of Synchrotron Radiation,* 18, 658-670, 2011.

[4] S. Sharma *et al*., "A Novel Design of High Power Masks and Slits", Proceedings MEDSI Conf. (MEDSI2014), Melbourne, Australia, October 2014.

* Work at the Advanced Photon Source is supported by the U. S. Department of Energy, Office of Science, Office of Basic Energy Sciences, under Contract No. DE-AC02-06CH11357.

† capatina@aps.anl.gov